Relationship between intracellular calcium and its muffling measured by calcium iontophoresis in snail neurones

Christof J. Schwiening and Roger C. Thomas

Department of Physiology, School of Medical Sciences, University of Bristol, Bristol BS8 1TD, UK

1. We have measured intracellular free calcium ion concentration ($[Ca^{2+}]_i$) with fura-2, and intracellular chloride with chloride-sensitive microelectrodes, in voltage-clamped snail neurones. By making iontophoretic injections of $CaCl_2$ we have investigated calcium muffling, the sum of the processes which minimize the calcium transient, at different values of $[Ca^{2+}]_i$.

2. By injection of calcium into cell-sized droplets of buffer we measured the calcium transport index. It was stable over the range pCa 6–7·4 (0·48 ± 0·06 measured at pCa 6·70 ± 0·12, $n = 5$).

3. Measurement of intracellular chloride activity during a series of fura-2–KCl pressure injections revealed a nearly linear relationship between fura-2 Ca^{2+}-insensitive fluorescence and the sum of the increments in intracellular chloride. This allowed us to calculate the intracellular fura-2 concentration ($[fura\text{-}2]_i$).

4. The rate of recovery of $[Ca^{2+}]_i$ following a depolarization-induced load was increased by low $[fura\text{-}2]_i$ (10–20 μM) but decreased by higher $[fura\text{-}2]_i$ (40–80 μM). These effects are consistent with the addition of a mobile buffer to the cytoplasm.

5. Iontophoresis of Ca^{2+} at various membrane potentials allowed us to calculate the intracellular calcium muffling power (the amount of calcium required to cause a transient tenfold increase in $[Ca^{2+}]_i$ per unit volume) and calcium muffling ratio (number of Ca^{2+} ions injected divided by the maximum increase in $[Ca^{2+}]_i$ per unit volume) at different values of $[Ca^{2+}]_i$.

6. Calcium muffling power at resting $[Ca^{2+}]_i$ was ~40 μM Ca^{2+} (pCa unit)$^{-1}$, (about 250 times less than for hydrogen ions). It increased linearly about fivefold with $[Ca^{2+}]_i$ over the range 20–120 nM (10 cells, 153 measurements) and therefore exponentially with decreasing pCa.

7. The calcium muffling ratio appeared to be constant (361 ± 14, $n = 10$ cells, 130 measurements) over the range 20–120 nM Ca^{2+}.

8. In three experiments we modelled the additional calcium buffering power produced by multiple pressure injections of fura-2 into voltage-clamped snail neurones. Back-extrapolation of the increases in calcium buffering power allowed us to calculate the calcium muffling power of the neurones.

9. Small increases in $[fura\text{-}2]_i$ (~10 μM) significantly increased intracellular calcium muffling power in individual experiments. However, the variability among neurones in intracellular calcium muffling power was large enough to obscure the additional buffering produced by fura-2 in pooled experiments.

Neuronal intracellular calcium ion concentration ($[Ca^{2+}]_i$) is maintained at a low level of about pCa 7·4 (~50 nM) by a variety of mechanisms, most importantly the calcium–hydrogen pump (Schwiening, Kennedy & Thomas, 1993). Consequently, a small Ca^{2+} influx through channels, or release from stores, can cause large increases in $[Ca^{2+}]_i$. Such increases are important in a range of cellular signalling mechanisms. The size of the increase in $[Ca^{2+}]_i$ will depend upon the combined effect of uptake or release by organelles, extrusion from the cell, diffusion and binding to cytoplasmic buffers. This combined effect is to reduce, or muffle, the rise in $[Ca^{2+}]_i$ compared with that which would occur in water.

Hitherto the ability of the cell to minimize increases in free Ca^{2+} has been expressed in two fashions. The first way is as the ratio of the number of ions remaining free to the

total number of ions added (Hodgkin & Keynes, 1957). The inverse of this ratio minus one was later defined as the 'calcium binding capacity' (Neher & Augustine, 1992). The second way is by analogy with hydrogen ion buffering power, the 'calcium buffering power', defined as the number of moles of calcium needed to produce a tenfold change in $[Ca^{2+}]_i$ per litre of cell volume. Although this second way might be considered as logarithmically distorted (Saleh, Rombola & Batlle (1991), it does allow easy comparison with hydrogen ion buffering.

Instead of the terms including buffering or binding, which strictly refer to calcium chelation by buffers, we prefer to use 'calcium muffling ratio' and 'calcium muffling power' to describe the ability of the cell to minimize increases in free Ca^{2+} (Thomas, Coles & Deitmer, 1991). We define the calcium muffling ratio as the number of Ca^{2+} ions injected divided by the maximum (peak) number appearing free. The calcium muffling power is defined as the amount of calcium injected which causes a transient tenfold increase in $[Ca^{2+}]_i$. Thus the calcium muffling ratio and power include not only the true chemical calcium buffering, but also the other physiologically relevant processes. Because of this, the techniques used will influence the values obtained.

Early attempts at measurement of calcium buffering were made over long time periods (Hodgkin & Keynes, 1957; Brindley, Tiffert, Scarpa & Mullins, 1977). They gave little information about the relationship between calcium buffering and intracellular free calcium and none about physiological calcium muffling. Ahmed & Connor (1988), working on molluscan neurones, estimated that endogenous calcium buffering power was around 40 μM Ca^{2+} (pCa unit)$^{-1}$ and that calcium buffering power increased with increasing $[Ca^{2+}]_i$. However, the smallest increases in calcium that they measured were outside what is now known to be the physiological range. Müller, Partridge & Swandulla (1993) have also made measurements of calcium buffering power in molluscan neurones. They estimated the amount of calcium entry on depolarization and reported a calcium buffer ratio of around 500, which did not vary up to calcium concentrations of 1 μM. It is not clear how their buffering ratio measurements relate to the buffering power measurements made by Ahmed & Connor (1988).

Measurements of whole-cell neuronal calcium buffering have been made in molluscan neurones (Belan, Kostyuk, Snitsarev & Tepikin, 1993), cultured dorsal root ganglion cells (Werth, Zhou, Nutter & Thayer, 1994) and adrenal chromaffin cells (Neher & Augustine, 1992; Zhou & Neher, 1993). There have been a few studies on nerve preparations (Fontana & Blaustein, 1993; Stuenkel, 1994) and some mathematical models of intracellular calcium buffering power (Sala & Hernandez-Cruz, 1990; Blumenfeld, Zablow & Sabatini, 1992; Nowycky & Pinter, 1993).

Most measurements of calcium buffering over a range of $[Ca^{2+}]_i$ have been made using the whole-cell patch-clamp technique, which involves some cell dialysis and a much altered intracellular and extracellular environment. Measurements of calcium buffering have also been made at highly elevated calcium levels and using large calcium transients. It is not clear how these disturbances affect normal calcium buffering.

We have investigated the buffering effects of incremental fura-2 pressure injections on snail neurones voltage clamped using conventional microelectrodes and therefore minimal dialysis. We have measured the effects of modest increases in $[\text{fura-2}]_i$ on recovery from depolarization. Rather than estimating the amount of calcium entering through voltage-gated channels, we have measured calcium muffling power and ratio using calibrated small iontophoretic injections of calcium at a physiological range of $[Ca^{2+}]_i$. We have thus been able to describe the relationship between calcium muffling and $[Ca^{2+}]_i$. In three experiments we have also been able to model the calcium buffering produced by incremental fura-2 pressure injections and to calculate the intrinsic calcium muffling power. Portions of this work have been published in a preliminary form (Schwiening, Kennedy & Thomas, 1995).

METHODS

Dissection

The circumoesophageal ganglion was isolated from the common snail, *Helix aspersa*, mounted in the experimental chamber and neurones exposed with a fine tungsten wire under snail Ringer solution (Kennedy & Thomas, 1995).

Solutions

All solutions were nominally bicarbonate free and were superfused at a rate of ~0·75 ml min^{-1} at room temperature (18–22 °C). The normal snail Ringer solution contained (mM): NaCl, 80; KCl, 4; $CaCl_2$, 7; $MgCl_2$, 5; and Hepes, 20. pH was adjusted to 7·5 by the addition of NaOH.

Intracellular buffer solution used in the droplet experiments contained (mM): KCl, 77·5; KOH, 22·5; NaCl, 5; $MgCl_2$, 1; Hepes, 10; BAPTA, 3·56; and fura-2, 0·01. The solution was titrated to pCa 8 with Ca-BAPTA and adjusted to pH 7·4 by addition of a small quantity of HCl (McGuigan, Lüthi & Buri, 1991). The *in vitro* calibration solutions were the same as the intracellular buffer solutions except they were made to pCa 5·5, 6, 6·5, 7, 7·5 and 8 using the method of McGuigan *et al.* (1991) (see Kennedy & Thomas, 1995).

Microelectrodes

Conventional. These were made from filamented borosilicate capillaries (2 mm in diameter, 75 mm in length; Clark Electromedical, Pangbourne, UK) pulled on a home-made vertical puller. The membrane potential-recording microelectrodes were filled with 1 M KCl containing 500 μM fura-2 (~10 MΩ). The calcium iontophoresis microelectrodes were filled with 100 mM $CaCl_2$ (~10 MΩ). The voltage-clamp microelectrodes were filled with 2 M KCl (~20 MΩ), except during the chloride measurement experiments where they were filled with 2 M potassium acetate. All conventional microelectrodes were dipped in waterproof black ink (Rotring, Hamburg, Germany) to make the tips visible.

Ion-sensitive microelectrodes. These were used in droplets to measure pCa and in cells to measure $[Cl^-]_i$. The ion-sensitive microelectrodes were made from unfilamented borosilicate glass (2 mm in diameter, 75 mm in length; Clark Electromedical) pulled on a home-made vertical puller (tips < 1 μm in diameter). The micropipettes were silanized as previously described by Kennedy & Thomas (1995). The silanized micropipettes were back-filled with normal snail Ringer solution for chloride measurements or 0·1 M $CaCl_2$, 100 mM KCl for calcium measurements. The back-fill solution was then forced to the tip with pressure, using a 25 ml syringe. If the micropipettes were blocked or showed no signs of hydrophobicity they were rejected. The chloride-sensitive microelectrodes were front-filled with Chloride Micro Exchanger (Cat. no. 477913, Corning, MA, USA) to form a 200 μm column. The calcium-sensitive microelectrodes were made as described by Kennedy & Thomas (1995) but their tips were broken to ~10 μm. All microelectrodes were used soon after filling.

Fluorescence measurement of $[Ca^{2+}]_i$

Fibre-optic set-up. Light from a 75 W xenon arc lamp was filtered (340, 360 and 380 nm) using a rotating wheel (30 Hz; Cairn Research, Faversham, UK) and collected by a fibre-optic light guide (Thomas & Schwiening, 1992). The other end of the guide was placed within 100 μm of the cell or the place where the droplet was to be injected, so as to illuminate it. A second light guide, connected to a filter (long-pass, > 510 nm) and photomultiplier tube (PMT), was placed next to the illuminating one. The voltage on the PMT was increased to 550 V for the droplet experiments or between 550 and 700 V, when using cells, to obtain a fluorescence signal of 1 V from either the 340 or 380 nm light. This level of fluorescence was recorded as the background and was subtracted from the total fluorescence recorded during the experiment. The cell or droplet was then impaled with the membrane potential microelectrode, voltage-clamp microelectrode, calcium-iontophoresis microelectrode or chloride-sensitive microelectrode when used. Neurones were voltage clamped at either −50 or −60 mV, typically requiring a current of ~2 nA. A 7 nA backing-off current was passed through the calcium iontophoresis microelectrode to prevent the passive leakage of calcium into the cell. Pressure (20–200 ms at 130–280 kPa) was briefly applied to the back of the membrane potential microelectrode to inject fura-2 into the cell. Calcium was injected iontophoretically using a high-voltage current clamp (S-7061A; World Precision Instruments, New Haven, CT, USA). Microelectrodes and light-guides were manoeuvred using Prior (Cambridge, UK) micromanipulators. The preparation was viewed through a horizontally mounted dissection microscope and voltages were recorded using conventional high-impedance amplifiers. Data were filtered (8-pole Bessel) and recorded at 4 Hz onto a PC through a CED interface and data collection program (Cambridge Electronic Design, Cambridge, UK). For more details of the apparatus see Kennedy & Thomas (1995).

Calibration of the ion-sensitive signals

The chloride-sensitive microelectrodes were calibrated using a two-point calibration. Calcium-sensitive microelectrodes were calibrated using the intracellular-like pCa 8 and pCa 7 solutions (McGuigan *et al.* 1991) and gave responses of 27–29 mV (pCa unit)$^{-1}$. In the droplet experiments the calcium-sensitive microelectrode voltage was used to calibrate the fura-2 ratio. An *in vitro* calibration was used for the fura-2 signals from snail neurones (H. J. Kennedy & R. C. Thomas, in preparation). Briefly, at the end of each day of experiments the fluorescence ratios of intracellular-like solutions of pCa 6, 6·5, 7, 7·5 and 8 were measured. A least-squares fit of the equation below was used to derive the calibration parameters.

$$\mathrm{pCa} = \mathrm{p}K_{\mathrm{app}} - \log\left(\frac{r - r_{\mathrm{min}}}{r_{\mathrm{max}} - r}\right),$$

where $\mathrm{p}K_{\mathrm{app}}$ was the apparent pK of fura-2 (typically ~5·65), r the ratio of 340 nm excited fluorescence against 380 nm excited fluorescence, r_{min} the minimum fluorescence ratio (typically ~0·11) and r_{max} the maximum fluorescence ratio (typically ~2·55). The above equation and derived parameters were then used to transform the fura-2 fluorescence measurements to pCa.

Throughout this paper $[Ca^{2+}]$ is used to denote the concentration of free calcium ions (following Alvarez-Leefmans, Rink & Tsien, 1981). As long as the ionic strength is constant, this will be directly proportional to the calcium activity. The calcium activity coefficient is unknown. pCa is taken to be $-\log[Ca^{2+}]$.

Calculation of rates

Rates were calculated by differentiating the sum of two exponentials fitted to the raw data by least-squares.

Statistics

Means are reported ± S.E.M. Significance is reported using Student's unpaired t test.

Measurement of transport index in droplets

In order to calculate the amount of calcium iontophoretically injected, it is necessary to know the transport index. The transport index for calcium is known to vary greatly depending upon the microelectrode used and the experimental conditions (Belan *et al.* 1993).

The flux (q, in M s^{-1}) of an ion species from a microelectrode during iontophoresis is given by:

$$q = \frac{\mathrm{TI} \times I}{zF}, \tag{1}$$

where TI is the transport index for the ion, z its valency, F the Faraday constant and I the current (see Purves, 1981).

The amount of calcium (Q_{Ca}) injected iontophoretically is therefore:

$$Q_{\mathrm{Ca}} = \frac{\mathrm{TI} \times It}{2F}, \tag{2}$$

where t is the duration of the injection. Re-arranging eqn (2):

$$\mathrm{TI} = \frac{Q_{\mathrm{Ca}} \times 2F}{It}, \tag{3}$$

Q_{Ca} can be calculated from the step change in Ca^{2+} (ΔpCa and $\Delta[Ca^{2+}]$) of a solution of known volume (v) and calcium buffering power.

The term calcium buffering power (β_{Ca} in M Ca^{2+} (pCa unit)$^{-1}$) was first used by Ahmed & Connor (1988). By analogy with pH buffering, we express it mathematically as:

$$\beta_{\mathrm{Ca}} = -\left(\frac{Q_{\mathrm{Ca}} - \Delta[Ca^{2+}] \times v}{v \times \Delta\mathrm{pCa}}\right). \tag{4}$$

Re-arranging gives:

$$Q_{\mathrm{Ca}} = (\Delta[Ca^{2+}] - \beta_{\mathrm{Ca}} \times \Delta\mathrm{pCa}) \times v. \tag{5}$$

Substituting eqn (5) into eqn (3) gives:

$$\mathrm{TI} = \frac{(\Delta[Ca^{2+}] - \beta_{Ca} \times \Delta\mathrm{pCa}) \times 2Fv}{It}. \quad (6)$$

By analogy with hydrogen ion buffering power, as shown by Koppel and Spiro in 1914 (cited by Roos & Boron, 1980), the calcium buffering power of a buffer with one calcium binding site is given by the equation:

$$\beta_{Ca} = \frac{[\mathrm{Buffer}] \times \ln 10 [Ca^{2+}] \times k_d}{([Ca^{2+}] + k_d)^2}, \quad (7)$$

where k_d is the dissociation constant of the calcium buffer.

Substituting eqn (7) into eqn (6):

$$\mathrm{TI} = \left(\Delta[Ca^{2+}] - \left(\frac{[\mathrm{Buffer}] \times \ln 10 [Ca^{2+}] \times k_d \times \Delta\mathrm{pCa}}{([Ca^{2+}] + k_d)^2}\right)\right) \times \frac{2Fv}{It}. \quad (8)$$

We have calculated the transport index during iontophoretic calcium injections, using eqn (8), by measuring the change in calcium concentration of a buffer solution of known volume and buffer concentration. Briefly, a volume of pCa 8 intracellular buffer solution (0·5–65 nl) containing 20 μM fura-2 was injected through a broken micropipette onto a pinhead in a non-fluorescent mineral oil. Three microelectrodes were placed inside the droplet: a conventional microelectrode connected to earth, a calcium-sensitive microelectrode (tip, ~10 μm) and a calcium iontophoresis microelectrode (filled with 100 mM $CaCl_2$). The two fibre-optic light guides were positioned around the droplet. The calcium-sensitive microelectrode signal was used to check the *in vitro* calibration values of the fura-2 ratio. A comparison of the two signals can be seen in Fig. 1*A*.

The steps on the pCa trace mark each iontophoretic injection of calcium. The calcium transport index is shown plotted against pCa in Fig. 1*B*. The transport index appears stable over the range pCa 6–7·4. Changing both the duration of the iontophoretic injection (0·5–10 s) and the size of the injection (5–20 nA) had no effect on the transport index under our experimental conditions. The transport index calculated from five experiments at pCa 6·70 ± 0·12 was 0·48 ± 0·06.

Calculation of intracellular muffling power

The calcium muffling power was calculated for transient changes in calcium using the equation:

$$\text{Calcium muffling power} = -\frac{(Q_{Ca} - \Delta[Ca^{2+}]_i \times v)}{v \times \Delta\mathrm{pCa}_i}. \quad (9)$$

The $\Delta\mathrm{pCa}_i$ and $\Delta[Ca^{2+}]_i$ were measured, the volume of the cell (v) calculated, assuming the cell to be a sphere, and Q_{Ca} was calculated from eqn (2) using the experimentally determined TI (0·48). The calcium muffling ratio was calculated from Q_{Ca}, v and $\Delta[Ca^{2+}]_i$:

$$\text{Calcium muffling ratio} = \frac{Q_{Ca}}{\Delta[Ca^{2+}]_i \times v}. \quad (10)$$

The intrinsic calcium muffling power was calculated by subtracting the theoretical fura-2 buffering power ($\beta_{\text{fura-2}}$, calculated using eqn (7)) from the total calcium muffling power (eqn (9)). $\beta_{\text{fura-2}}$ is dependent upon $[\text{fura-2}]_i$, which was calculated from the change in the total calcium buffering power following a fura-2 pressure injection. Assuming a linear relationship between $[\text{fura-2}]_i$ and fluorescence intensity when excited with 360 nm light, it was therefore possible to calculate the intrinsic calcium muffling power for three cells.

RESULTS

Intracellular fura-2 concentration

Since fura-2 is a buffer as well as an indicator, it will contribute to intracellular calcium muffling. Thus we needed to measure the fura-2 levels used in our

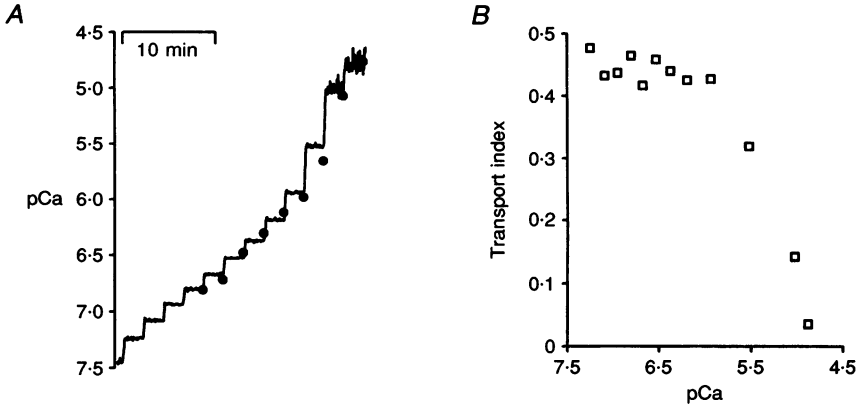

Figure 1. Calculation of the calcium transport index in a droplet

A, a droplet (175 μm diameter) of intracellular-like solution containing 3·58 mM BAPTA and 10 μM fura-2 was injected under non-fluorescent oil onto a pinhead. The droplet was earthed using a 3 M KCl microelectrode and illuminated with a cycle of 340, 360 and 380 nm light. Fluorescence was collected by a second fibre optic and detected by a photomultiplier tube. The continuous trace shows the fura-2 ratio calibrated for pCa. A calcium-sensitive microelectrode (data shown by circles) and a microelectrode filled with 100 mM $CaCl_2$ were also placed into the droplet. Twelve iontophoretic injections of calcium were made into the droplet (34 nA for 10 s). The fura-2 ratio was calibrated *in vitro* using the same solutions as used to calibrate the calcium-sensitive microelectrode. *B*, plot of transport index against pCa calculated from Fig. 1*A*.

experiments. We did this by making multiple pressure injections of small but unknown amounts of a solution containing fura-2 and KCl into snail neurones whilst measuring $[Cl^-]_i$ with ion-sensitive microelectrodes. From the step changes in $[Cl^-]_i$ following the pressure injections we have calculated the amount of fura-2 added to the cell. Figure 2 shows an example of such an experiment.

A neurone was impaled with three microelectrodes: one to measure membrane potential (E_m) and to pressure inject fura-2–KCl, another to voltage clamp the neurone, and an ion-sensitive microelectrode to measure $[Cl^-]_i$. The ratio of fluorescence from fura-2 (> 510 nm) excited at 340 and 380 nm was used to monitor $[Ca^{2+}]_i$. The arrows mark ~0·5 s pressure injections of the 1 mM fura-2 in 1 M KCl. Each injection caused a rise in the $[Cl^-]_i$ and the isosbestic wavelength of fura-2 for calcium. Because $[Cl^-]_i$ tended to recover following each injection, whilst $[fura\text{-}2]_i$ did not, we have summed the step changes in $[Cl^-]_i$ to obtain the total added Cl^-. From the sum of the step changes in $[Cl^-]_i$ following each injection ($\Sigma[Cl^-]_i$), shown by the open squares on the lowest trace, we have calculated $[fura\text{-}2]_i$. Given that the injected Cl^- is presumably distributed in the same volume as the fura-2, this should be equal to $[fura\text{-}2]_i$ (μM). There is good agreement between $\Sigma[Cl^-]_i$ and the isosbestic signal for fura-2, suggesting that although $[Cl^-]_i$ is regulated, fura-2 is trapped within the cell. Thus in Fig. 2 the measurements of $[Ca^{2+}]_i$ were made at a $[fura\text{-}2]_i$ of ~10 to ~120 μM.

The effect of fura-2 on the calcium transients was assessed by repeatedly loading the neurone with calcium by depolarizing it. The neurone was held at −50 mV, but following each injection the membrane was depolarized to +7 mV for 1 s, three or four times. The fura-2 ratio trace shows the resulting calcium transient, which is presumably due mostly to calcium entry through voltage-activated channels.

The effect of increasing $[fura\text{-}2]_i$ on the calcium transients can be seen more easily in Fig. 3. In Fig. 3*A* we show two transients, indicated by asterisks in Fig. 2, on a faster time base. The dotted horizontal lines indicate the two fura-2 ratios, corresponding to two different values of $[Ca^{2+}]_i$, at which we analysed the rates of recovery. In Fig. 3*B* we have plotted these rates of recovery for all the transients in Fig. 2 against $[fura\text{-}2]_i$.

The rate of recovery of $[Ca^{2+}]_i$ at low $[Ca^{2+}]_i$ increased as $[fura\text{-}2]_i$ was increased to ~20 μM, consistent with the addition of a mobile calcium buffer increasing the rate of

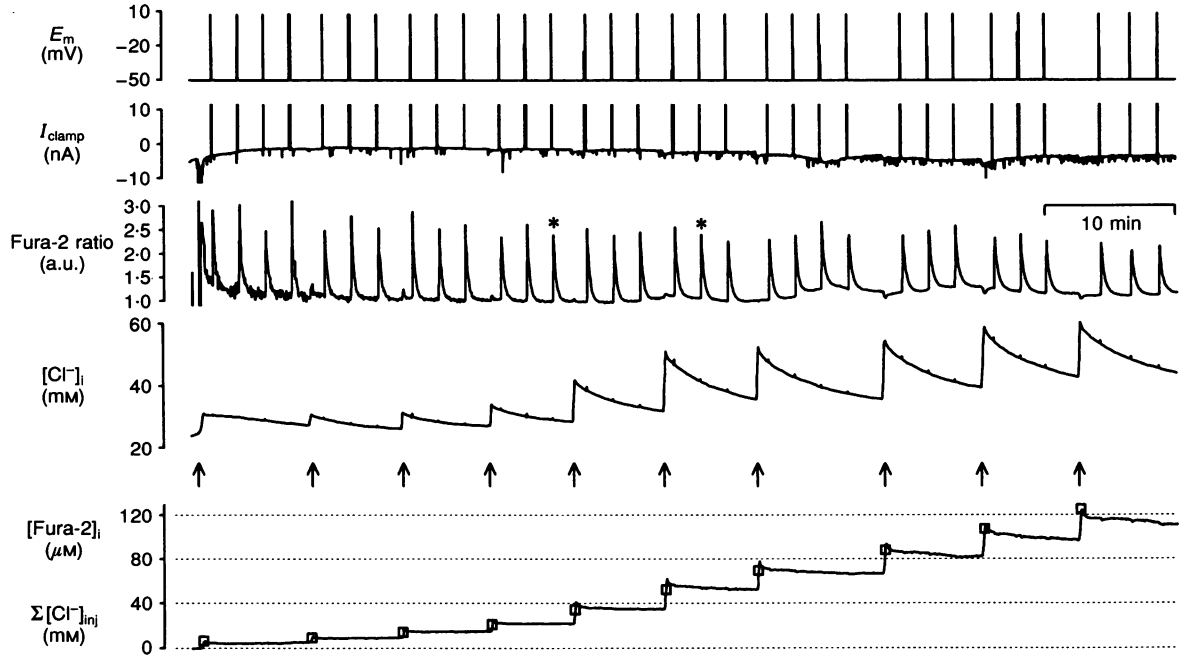

Figure 2. Chloride and $[Ca^{2+}]_i$ measurements during the pressure injection of fura-2 and KCl into a voltage-clamped snail neurone

Records of membrane potential (E_m), clamp current (I_{clamp}), fura-2 ratio, intracellular Cl^- ($[Cl^-]_i$), fura-2 calcium-insensitive fluorescence ($[fura\text{-}2]_i$) and the sum of the added Cl^- ($\Sigma[Cl^-]_{inj}$). The snail neurone was held at −50 mV and periodically depolarized to +7 mV for 1 s. Intracellular chloride was monitored using a chloride-sensitive microelectrode. The arrows indicate the pressure injection of KCl and fura-2. The open squares on the bottom trace show the total chloride injected into the neurone, as measured from the step changes in $[Cl^-]_i$. The continuous bottom trace shows the isosbestic Ca^{2+} signal for fura-2 (360 nm) calibrated using the sum of the chloride injected. Asterisks on the fura-2 trace mark transients plotted in Fig. 3*A*. Representative of 5 experiments.

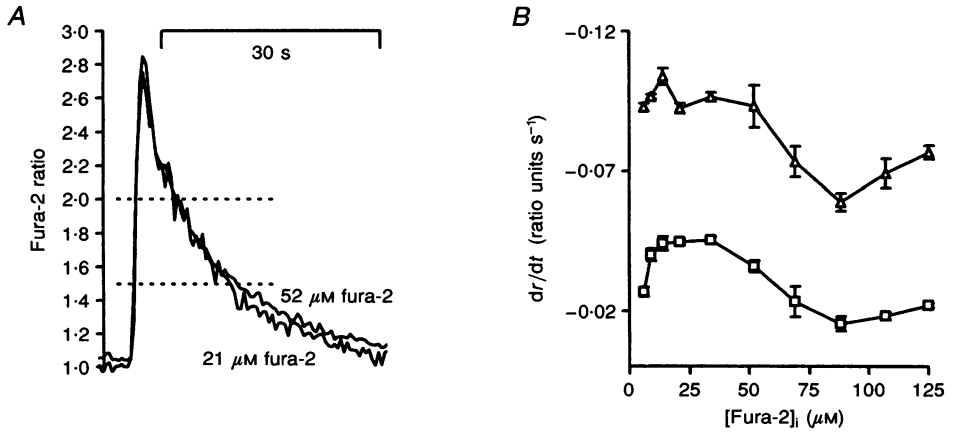

Figure 3. Rate of recovery of the fura-2 ratio following depolarization plotted against $[fura\text{-}2]_i$

A, the two depolarization-induced transients marked with asterisks in Fig. 2 are plotted at a sampling rate of 2 Hz. The dotted lines indicate the fura-2 ratios at which the rates of recovery were calculated for Fig. 2*B*. *B*, the recovery phase of the fura-2 transients following each of the 32 depolarizations in Fig. 2 was fitted with the sum of two exponentials. Rates of recovery at two fura-2 ratios (shown by dotted lines in Fig. 3*A*), for each of the 3 or 4 transients, at a given $[fura\text{-}2]_i$ were averaged and plotted against $[fura\text{-}2]_i$. △, fura-2 ratio, 2·0; □, fura-2 ratio, 1·5.

calcium mobility within the cell. The rate then remained stable with $[fura\text{-}2]_i$ in the range of 25–50 μM, and fell at levels over 50 μM. This fall in the rate of calcium recovery is expected as the higher levels of fura-2 increase the calcium buffering power. We therefore chose to use around 20–40 μM fura-2_i in our other experiments. This minimized the effect of $[fura\text{-}2]_i$ buffering on the calcium transient kinetics whilst still achieving a reasonable signal-to-noise ratio. The effects of fura-2 on calcium mobility may be avoidable by using fura-2 dextran, but we have not done this.

The effect of injecting the same amount of calcium at different rates

Before using calcium injection, at a point source, to measure intracellular calcium muffling power, it was necessary to test the effect of different injection parameters on the injection-evoked Ca^{2+} transients. Long injections

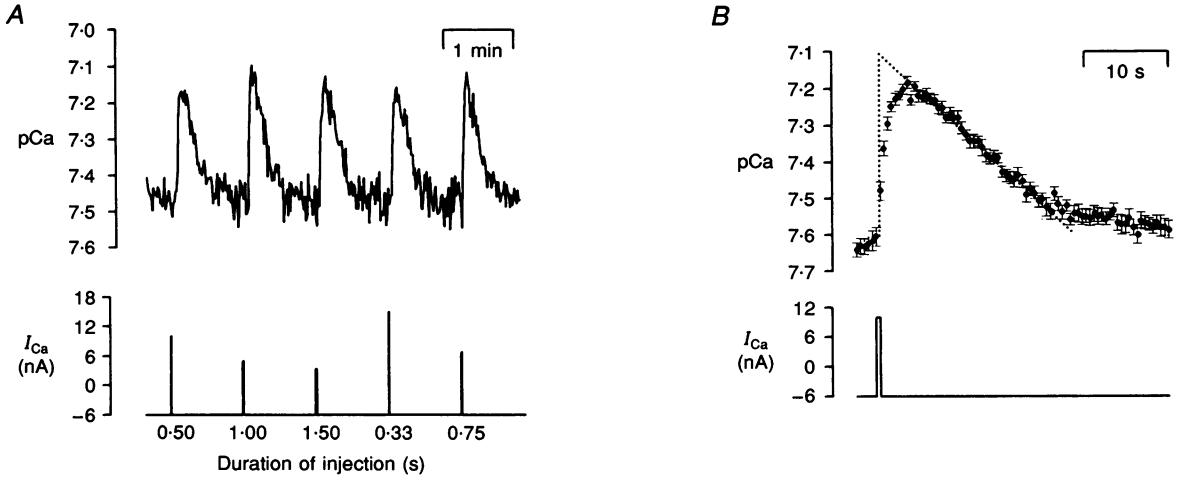

Figure 4. $[Ca^{2+}]_i$ transients produced by the injection of the same amount of charge at five different rates

A, a snail neurone was voltage clamped at −60 mV and pressure injected with fura-2 (~20 μM). At about 1 min intervals calcium was iontophoretically injected for the length of time shown. Each injection contained $\sim 1{\cdot}2 \times 10^{-14}$ mol of calcium. The mean calcium muffling power was 36 ± 1 μM Ca^{2+} (pCa unit)$^{-1}$ (muffling ratio, 315 ± 11) at pCa $7{\cdot}47 \pm 0{\cdot}01$ ($n = 5$). *B*, the average of 16 calcium transients (data from experiment shown in Fig. 8) produced by 0·5 s, 10 nA iontophoretic injections. Error bars represent S.E.M.; data shown at 2 Hz. Dotted lines show the size of the calcium transient expected had there been no calcium regulation.

might produce high muffling power values due to greater calcium regulation and large calcium injections might saturate the fura-2 signal or increase muffling power due to increased mitochondrial calcium uptake at the site of calcium injection. The intracellular $[Ca^{2+}]$ must also be in equilibrium throughout the cell. The effect of different sizes and durations of calcium injections on the calcium muffling power were therefore investigated. A typical result of an experiment, in which we injected the same amount of total charge over five different time periods (0·33–1·5 s, therefore at rates of between 2·2 and 45 nA s^{-1}), is shown in Fig. 4*A*.

A snail neurone was selected and impaled with a membrane potential microelectrode filled with KCl and 1 mM fura-2, a voltage-clamp microelectrode and a calcium iontophoresis microelectrode. Fura-2 was pressure injected into the cell to an estimated initial concentration of ~20 μM. After allowing the cell to recover for ~15 min we repeatedly iontophoresed calcium at different rates. The rise in pCa_i caused by each injection was similar (~0·3 pCa units) and the peak occurred several seconds after the start of the calcium injection. The complete recovery of $[Ca^{2+}]_i$, however, took almost 1 min. In Fig. 4*B* we show the average of sixteen calcium transients produced by 0·5 s, 10 nA iontophoretic injections of calcium. The peak change in $[Ca^{2+}]_i$ occurs about 2·5 s after the end of the calcium injection. This delay must represent the redistribution of injected calcium throughout the neurone. We have attempted to estimate the effect of calcium regulation by back-extrapolating the recovery of the calcium transient to the start of the calcium injection (dotted line in Fig. 4*B*). The time course for calcium equilibrium throughout the cell is faster than that for calcium extrusion, but calcium regulation has a small but significant effect on the calcium muffling power.

The effect of injecting three different amounts of calcium at the same rate on intracellular calcium buffering power

Although the injection of the same amount of calcium at different rates seems to have little effect on the size of the calcium transient, injecting larger amounts of calcium would obviously increase the size of the transient. If calcium muffling power is a steep function of $[Ca^{2+}]_i$, titrating calcium over this larger range would cause the

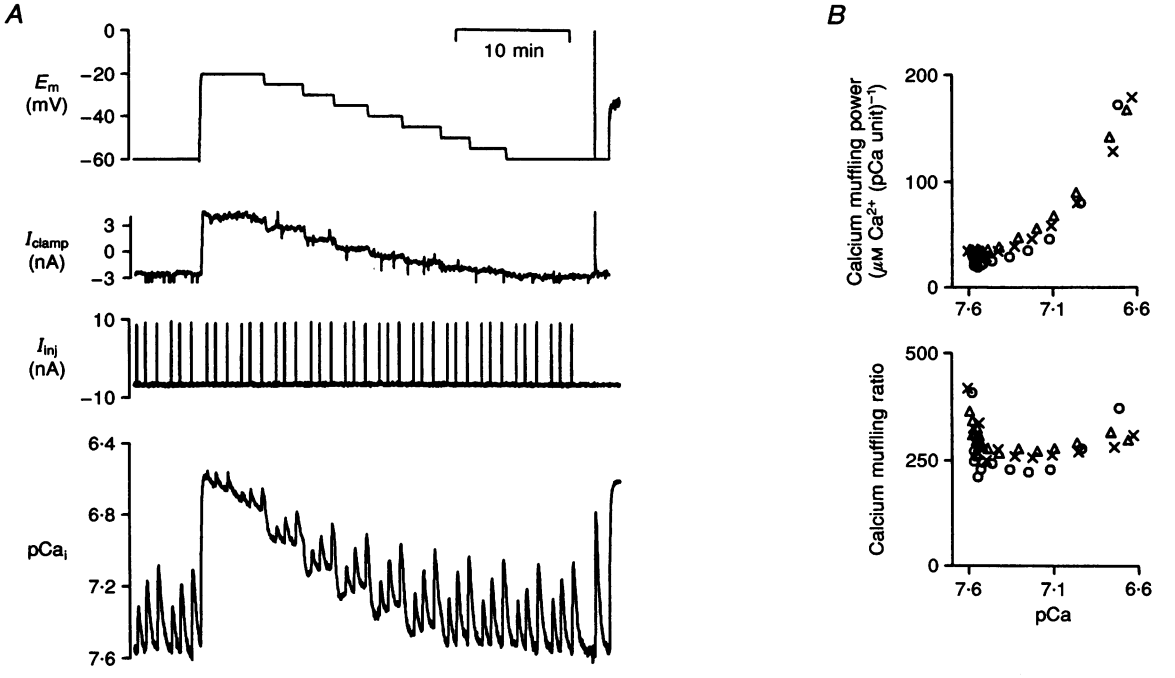

Figure 5. Intracellular calcium muffling power measured in a voltage-clamped snail neurone

A, an extract from an experiment in which a snail neurone was pressure injected with a small amount of fura-2 (estimated as 20–40 μM) and Ca^{2+} was repeatedly iontophoresed at different values of $[Ca^{2+}]_i$. At the start of the experiment the neurone was held at −60 mV and two cycles of three 10 nA calcium injections were made (0·5, 1 and 1·5 s). After about 6 min the neurone was depolarized to −20 mV and another two cycles of calcium injections were made. The neurone was then repolarized in 5 mV steps and at each potential another cycle of calcium injections was made. At the end of the experiment the neurone was depolarized to 0 mV for 1 s and then the voltage clamp was switched off and the cell was allowed to fire action potentials, which were not captured by the 4 Hz data recording system. *B*, graphs of calcium muffling expressed in two different ways against initial pCa calculated from the calcium transients in Fig. 5*A*. All injections were of 10 nA: ○, 0·5 s; ×, 1 s; △, 1·5 s.

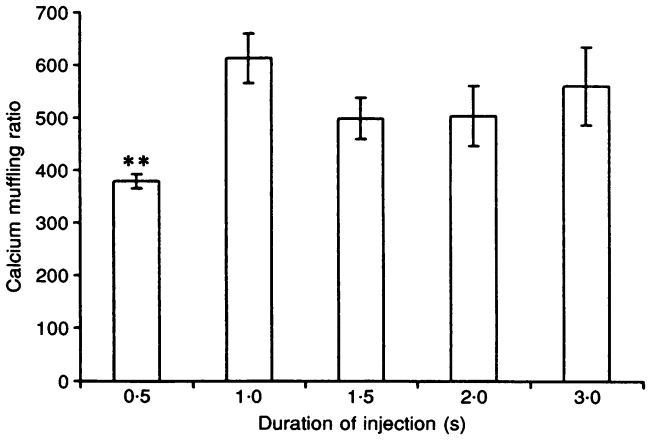

Figure 6. The effect of different amounts of calcium injected at the same rate on the calculated calcium muffling ratio

The calcium muffling ratio was calculated for calcium injections of 10 nA for 0·5, 1, 1·5, 2 and 3 s injections at a mean $[Ca^{2+}]_i$ of 60 nM in 11 neurones. The muffling ratio calculated from 0·5 s injections is significantly less than that from the longer injections. Error bars indicate S.E.M. $^{**}P < 0{\cdot}002$.

calcium muffling power to appear to be greater than that calculated with smaller calcium injections. We have therefore measured calcium muffling power by adding different but small amounts of calcium over a range of pCa_i values. Figure 5*A* shows an example of such an experiment.

The neurone (150 μm in diameter) was held at −60 mV and had a resting pCa_i of around 7·6. Two cycles of calcium injections (0·5, 1 and 1·5 s in duration) of size 10 nA were made. It can be seen that each iontophoretic injection was accompanied by a rise in calcium. We then depolarized the neurone to −20 mV, causing an increase in pCa_i, presumably owing to the opening of voltage-activated calcium channels. We then repeated the two cycles of calcium injections. The neurone was then stepped back to the holding potential in 5 mV steps. At each step a cycle of calcium injections was made. At about 2 min before the end of the experiment the cell was depolarized to 0 mV for 1 s to give an indication of the physiological range of calcium levels. The voltage clamp was then switched off and the cell fired action potentials (which were not apparent on the figure due to the slow time base). During this period the cell maintained a resting membrane potential of about −50 mV and fired action potentials at a rate of ~2 Hz to ~+20 mV. Intracellular calcium increased to around pCa 6·5 during this period of action potentials.

We measured the change in intracellular calcium caused by each calcium injection and, knowing the calcium transport index, duration and size of each injection, the cell volume and pCa_i, we were able to calculate the calcium muffling power and ratio for each injection. These values are plotted in Fig. 5*B* in two ways. First, by analogy with hydrogen ion buffering power, we plotted these values as the microequivalents of calcium needed to transiently change the pCa of one litre of cell fluid by 1 pCa unit, against the initial pCa before the injection. We have plotted calcium muffling for the 0·5, 1 and 1·5 s injections. The relationship of the calcium muffling power is close to exponential for all of the injection lengths. Calcium muffling power appears to be greater following the larger injections of calcium (Fig. 5*B*, △), as one would expect for such a relationship of intracellular calcium muffling power with pCa. Second, we have also plotted the calcium muffling ratio against initial pCa in Fig. 5*B*. The relationship between the calcium muffling ratio and pCa is nearly flat. However, the longer injections give slightly elevated ratios.

In Fig. 6 we show the mean data from eleven neurones where the calcium muffling ratio was measured following 0·5, 1, 1·5, 2 and 3 s calcium injections of 10 nA at a mean $[Ca^{2+}]_i$ of 60 nM.

The muffling ratio is significantly smaller ($P < 0{\cdot}002$) for the 0·5 s injections. Therefore, calcium injections used to measure calcium buffering or muffling should be as small as is consistent with a reasonable signal-to-noise ratio.

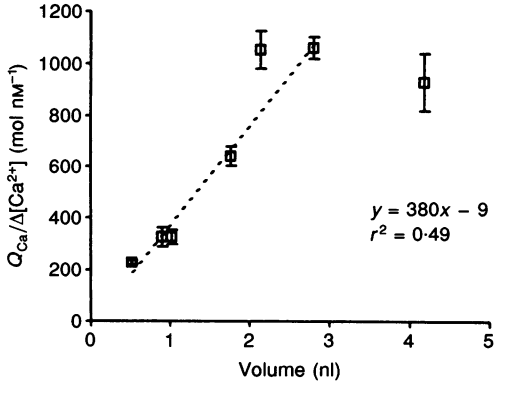

Figure 7. The relationship between the quantity of calcium injected for a given change in $[Ca^{2+}]_i$ and cell volume

The amount of calcium injected divided by the change in $[Ca^{2+}]_i$ was calculated and the mean (± S.E.M.) was plotted against cell size. Data are shown for $[Ca^{2+}]_i$ in the range 20–120 nM and for 10 nA iontophoretic injections of 0·5 s duration in normal Ringer solution. One hundred and thirty-eight data points are included in the mean values from 11 neurones. The dotted line is a least-squares fit to data for cell sizes up to 4 nl.

Effect of cell size on calcium muffling power

The neurones used in this study varied in diameter (100–200 μm). Although unlikely, it is possible that calcium muffling power is related to cell size. We therefore calculated calcium muffling power for a range of differently sized neurones. The cell volume was calculated by assuming the cells to be perfect spheres, although they were frequently not and the diameter was hard to determine accurately. We have therefore plotted the quantity of calcium injected into the cell divided by the change in $[Ca^{2+}]_i$ against cell volume in Fig. 7, thereby confining the volume errors to the x-axis.

If the data fit on a straight line then muffling power is independent of cell volume. The gradient of the least-squares fit line shown in Fig. 7 is 380 and is the mean calcium muffling ratio. Although there is considerable scatter within the data, it seems that calcium muffling is not highly dependent on cell volume up to 4 nl. The largest cell that was injected with calcium, which is not included within the fit, appears to have a lower calcium muffling ratio than would be extrapolated from the fitted line.

Calculation of endogenous calcium muffling power by extrapolation

To calculate the endogenous calcium muffling power, we have modelled the buffering power due to the additions of the calcium buffer fura-2 and then back-extrapolated to zero added fura-2. We have done this because we cannot measure calcium muffling without adding fura-2. In

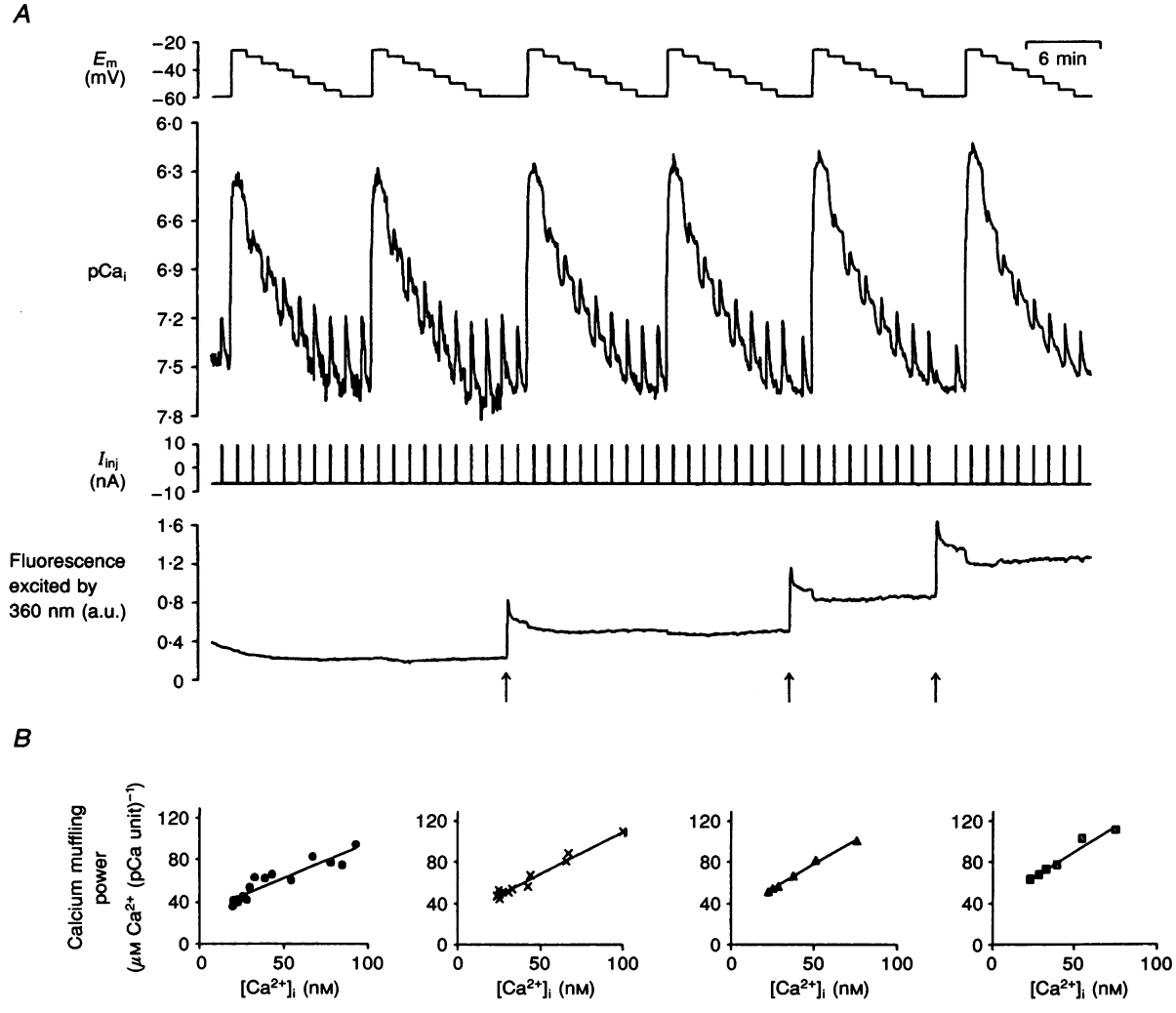

Figure 8. Calcium muffling power calculated from iontophoretic calcium injections at different values of $[Ca^{2+}]_i$ and [fura-2]$_i$

A, an extract from an experiment in which a snail neurone was voltage clamped and injected with a small quantity of fura-2 before the start of the recordings shown in the figure. The cell was initially held at −60 mV and calcium was iontophoresed at intervals. The cell was depolarized to −25 mV and then repolarized back to −60 mV in 5 mV steps six times. Three injections of fura-2 were also made into the neurone (marked by the vertical arrows). *B*, calcium muffling power plotted against $[Ca^{2+}]_i$ for each of the four values of [fura-2]$_i$; data from Fig. 8*A*. Data were fitted with straight lines.

Fig. 8*A* we show an example of an experiment designed to measure calcium muffling power over a range of pCa_i values following incremental fura-2 pressure injections. A snail neurone was selected, impaled with an E_m microelectrode and a voltage-clamp microelectrode. It was then held at −60 mV and injected with what we estimated to be a small amount of fura-2 (< 20 μM). The cell was also impaled with a calcium iontophoresis microelectrode, clamped at −60 mV for a few minutes and then depolarized to −25 mV and repolarized in steps of 5 mV to −60 mV. At each potential, calcium was iontophoresed at 10 nA for 0·5 s. Following two cycles of depolarization, more fura-2 was pressure injected into the neurone. The neurone was then depolarized and injected repeatedly with calcium. Following two more cycles of depolarization, more fura-2 was added to the cell. Again the cell was depolarized and injected with calcium. Finally, another fura-2 injection was made and the cell depolarized and injected with calcium again.

Figure 8*B* shows the calculated calcium muffling power plotted against $[Ca^{2+}]_i$ for the four increasing levels of fura-2. The data were plotted against $[Ca^{2+}]_i$ (nM) rather than pCa_i to give a linear function rather than an exponential (see Fig. 5*B*). Each graph in Fig. 8*B* has been fitted with a least-squares straight line.

In Fig. 9*A* we have replotted the four straight lines on one graph. As fura-2 increases, the lines increase in slope and are shifted upwards. We then attempted to account for the increases in muffling power by adding a contribution of buffering due to fura-2. The initial set of data from Fig. 8*B*, for the lowest $[fura\text{-}2]_i$, was then transposed to fit the next set of data produced by the subsequent incremental injection of fura-2 by the addition of the theoretical buffering of an amount of fura-2, as given by eqn (7). The best least-squares fit of this transposition to the original data was achieved by adding the buffering of 20 μM fura-2 and is shown in Fig. 9*A* by the lowest dotted line. This procedure was repeated for the next two incremental fura-2 injections. It can be seen in Fig. 9*A* that the final set of data from Fig. 8*B* is fitted well by the addition of the buffering of 80 μM fura-2. In Fig. 9*B* we have plotted the calculated added $[fura\text{-}2]_i$ against the average 360 nm signal. The data points have been fitted with a straight line, indicating that the 360 nm signal is proportional to the $[fura\text{-}2]_i$ and that it is therefore possible to extrapolate back to the background 360 nm fluorescence.

In Fig. 9*C* we have plotted the straight line fit to the initial set of data from Fig. 8*B* (continuous line) and the same data minus the buffering power of the apparent initial $[fura\text{-}2]_i$ (18 μM; dotted line) from back-extrapolation in

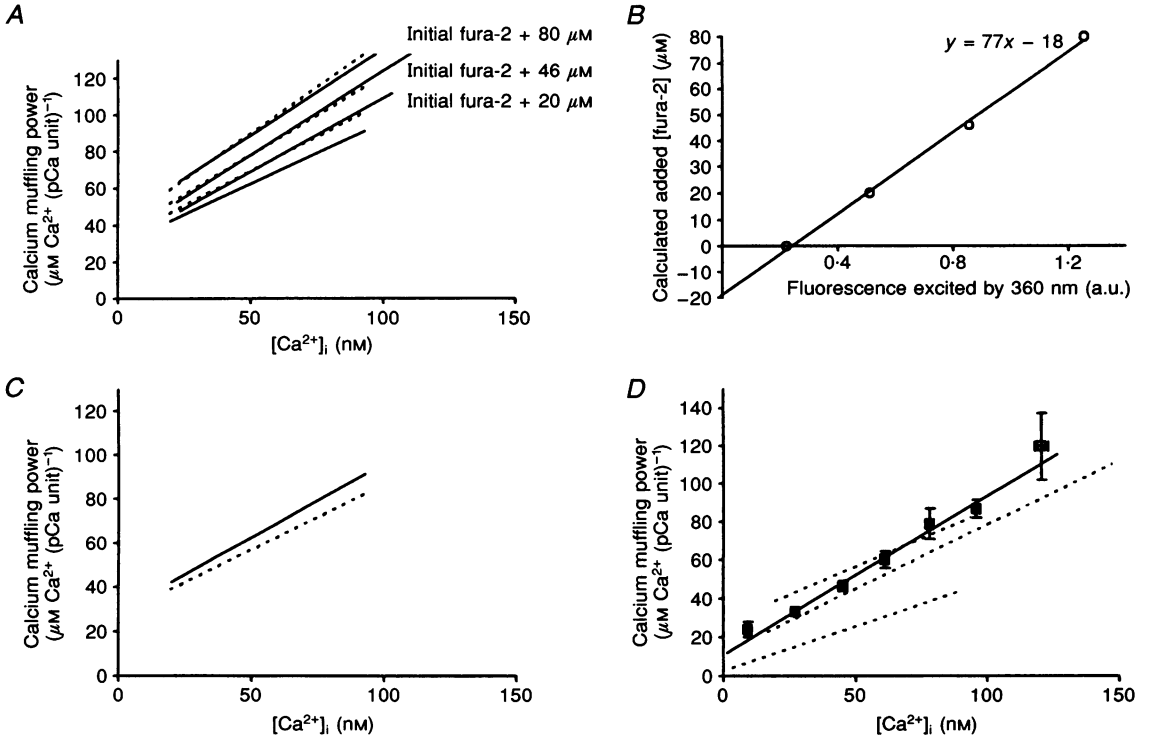

Figure 9. Calculation of endogenous calcium muffling power against $[Ca^{2+}]_i$

A, least-squares lines for calcium muffling power against $[Ca^{2+}]_i$ for different values of $[fura\text{-}2]_i$. *B*, calculated $[fura\text{-}2]_i$ from the increase in calcium muffling power plotted against 360 nm excited fluorescence. *C*, extrapolated calcium muffling power against $[Ca^{2+}]_i$ calculated from Fig. 9*A*. *D*, calcium muffling power plotted against $[Ca^{2+}]_i$ for 11 neurones (n = 15, 47, 33, 25, 13, 11, 5 for data points) containing minimal fura-2 and for three neurones (dotted lines) in which the buffering by fura-2 has been subtracted.

Fig. 9*B*. We have repeated this procedure for two other cells. In Fig. 9*D* we show three straight line fits representing the endogenous calcium muffling power from three cells (dotted lines). The continuous straight line is a least-squares fit to the pooled calcium muffling power data from eleven cells. These data were from cells with minimal $[fura\text{-}2]_i$, 0·5 s, 10 nA injections and are not corrected for the buffering of fura-2. There is considerable scatter in the individual data, but the mean calcium muffling power calculated with minimal fura-2 appears not to be significantly different from the pooled endogenous calcium muffling power.

DISCUSSION

In this study we have used small quantified calcium injections in the presence of low levels of fura-2 to measure calcium muffling over a range of values of $[Ca^{2+}]_i$ in neurones which have been minimally disturbed. We find that calcium muffling *power* (the amount of calcium required to cause a transient tenfold increase in $[Ca^{2+}]_i$) in snail neurones is highly dependent upon $[Ca^{2+}]_i$. The relationship between calcium muffling power (μM Ca^{2+} (pCa unit)$^{-1}$) and $[Ca^{2+}]_i$ (nM) can be described by the straight line $0{\cdot}8[Ca^{2+}]_i + 9$ over the $[Ca^{2+}]_i$ range 20–120 nM. The calcium muffling power at resting $[Ca^{2+}]_i$ (~40 nM) is 40 μM Ca^{2+} (pCa unit)$^{-1}$). On the other hand, we find that the calcium muffling *ratio* (number of Ca^{2+} ions injected divided by the maximum increase in $[Ca^{2+}]_i$) is constant with changes in $[Ca^{2+}]_i$. The mean calcium muffling ratio in our study was 361 ± 14 ($n = 10$ cells, 130 measurements) over the $[Ca^{2+}]_i$ range 20–120 nM.

Our ratio measurements are in broad agreement with other studies on molluscan neurones (Ahmed & Connor, 1988; Müller *et al.* 1993; Belan *et al.* 1993). The muffling ratio is the same as that published for *Helix pomatia* neurones (360 over the $[Ca^{2+}]_i$ range 200–300 nM) by Belan *et al.* (1993) and slightly lower than that reported for neurones from the same species (480 ± 70) by Müller *et al.* (1993). They are higher than those measured in both bovine chromaffin cells (40; Zhou & Neher, 1993) and rat secretory nerve ending (174; Stuenkel, 1994).

Ahmed & Connor (1988) described the relationship between calcium buffering power (μM Ca^{2+} (pCa unit)$^{-1}$) and $[Ca^{2+}]_i$ (nM) with a line of gradient of $0{\cdot}003[Ca^{2+}]_i + 45$, but they used calcium steps in excess of 9000 nM. They also assumed that calcium was restricted to diffusion shells and did not reach equilibrium. Surprisingly, the extrapolated resting level that they report is close to that which we found. Using the calcium clamp technique, Belan *et al.* (1993) report that isolated *Helix pomatia* neurones require 36 ± 20 μM Ca^{2+} per cell volume to increase $[Ca^{2+}]_i$ by 100 nM. Given their resting $[Ca^{2+}]_i$ of ~200 nM, we estimate that this is equivalent to about 200 μM Ca^{2+} (pCa unit)$^{-1}$). Although our study is concerned with lower $[Ca^{2+}]_i$ levels (20–120 nM), we would predict a similarly high muffling power at 200 nM Ca_i^{2+}.

There have been numerous attempts to measure intracellular calcium buffering power in neurones. Many of these studies were with the whole-cell patch-clamp technique, and most used the acetoxymethyl ester of fura-2 to measure calcium. The calcium loads were quantified by measuring the calcium current. Unfortunately, the whole-cell patch-clamp technique causes some dialysis of the normal cell contents. Thus the cell tends to lose not only mobile calcium buffers but also physiologically important molecules which affect calcium handling, such as ATP and $InsP_3$. High levels of fura-2 used in many studies contribute to calcium buffering and the membrane-permeable fura-2 loading technique presents problems in calibration of $[Ca^{2+}]_i$ (Zhou & Neher, 1993). Using the calcium current to quantify the calcium load necessitates the use of unphysiological Ringer solution (Na^+ free) and pipette solutions (K^+ free and calcium buffers). However, Zhou & Neher (1993) employed the nystatin-perforated patch technique to minimize intracellular dialysis, whilst Johnson & Byerly (1993) used flash-photolysis of caged calcium to produce calcium loads. Only a few others have used iontophoretic or pressure injections of calcium to estimate calcium buffering (Ahmed & Connor, 1988; Belan *et al.* 1993; Partridge, 1994).

In bovine adrenal chromaffin cells Zhou & Neher (1993) showed that calcium binding capacity did not change between 0·1 and 3 μM. However, those calculations were made by titrating calcium in relatively large steps. Indeed, many studies of calcium buffering present measurements of buffering at one level of intracellular calcium.

Our measurements of calcium muffling power were made assuming that calcium was in equilibrium throughout the cell several seconds after the end of the calcium injection. Calcium is known to diffuse slowly (~10^{-7} cm^2 s^{-1}) in cells. It is therefore possible that calcium gradients might exist within large neurones (> 100 μm) even after a second or more (Ahmed & Connor, 1988; Müller *et al.* 1993). This would lead to an underestimate of the neuronal muffling power in large cells, since some of the cytoplasm does not 'see' the calcium load. It is also known that quite low levels of fura-2 significantly increase the rate of calcium redistribution (Zhou & Neher, 1993). If the endogenous calcium buffers are immobile then this could be the explanation for the increase in the rate of calcium recovery seen in Fig. 3.

Our results are similar to those reported by Müller *et al.* (1993) on isolated neurones from *Helix pomatia*. Their neurones seem to have no visible axon and it is not clear how they were isolated. The isolation and loss of axon may have changed calcium muffling. From their Methods section it is also appears that the calcium transients and calcium currents were measured under different conditions

(i.e. with different clamp electrodes and different bathing solutions). Given that Na^+–Ca^{2+} exchange is thought to be present in some isolated snail neurones (Kostyuk, Mironov, Tepikin & Belan, 1989), it is possible that the $[Ca^{2+}]_i$, and therefore calcium currents, measured in Na^+-free Ringer solution were not the same as those occurring whilst the fluorescence measurements were made. The measurements presented were also made with relatively high $[fura\text{-}2]_i$ (0·2–1 mM). Given these problems it is not surprising that they report resting calcium levels over a wide range (10^{-8}–10^{-7} M).

The nature of the calcium muffler

It is not clear what proportion of the muffling power that we have measured is due to actual cytoplasmic calcium buffering and what is due to other mechanisms such as sequestration and regulation. From calcium-activated currents, Barish & Thompson (1983) reported that calcium muffling in molluscan neurones depends upon the site of the calcium load. They postulated that point source calcium injections would be spatially limited by mitochondria whilst calcium loads through the plasma membrane would be more uniform. They typically injected 280 nC of charge, which they estimated would cause a rise in $[Ca^{2+}]_i$ of 10–20 μM. Indeed, such calcium increases would be expected to be muffled by mitochondria (Meech & Thomas, 1980). More recent work by Partridge (1994) on *Helix* neurones also implicates mitochondria as the major sink for large (250 μmol of Ca^{2+} per litre of cell volume) injections of calcium. White & Reynolds (1995) report that in cultured cortical neurones calcium loads produced by exposure to glutamate or high K^+ are buffered completely by Na^+–Ca^{2+} exchange and mitochondrial calcium uptake. This highlights the problem of terminology, since they presumably use the term buffer to refer to calcium sequestration or extrusion and not chelation by buffers. The maximum $[Ca^{2+}]_i$ (120 nM) and calcium loads (~10 fmol Ca^{2+}) that we imposed in this study were at least an order of magnitude smaller than those previously studied. We suspect that such small calcium loads were buffered mainly by cytoplasmic proteins. However, it is possible that mitochondrial calcium uptake was responsible for a small proportion of the increase in calcium muffling power at raised $[Ca^{2+}]_i$. This is in agreement with Werth & Thayer (1994). Working on rat cultured dorsal root ganglion neurones, they showed that less than twenty-five action potentials caused no mitochondrial calcium uptake whilst $[Ca^{2+}]_i$ increased from ~100 to ~600 nM. Furthermore, given the time course of calcium extrusion from the cell by the Ca^{2+}–H^+ pump (Fig. 4*B*), it is possible that up to ~20% of the calcium muffling power was due to calcium regulation.

Ahmed, Z. & Connor, J. A. (1988). Calcium regulation by and buffer capacity of molluscan neurons during calcium transients. *Cell Calcium* **9**, 57–69.

Alvarez-Leefmans, F. J., Rink, T. J. & Tsien, R. Y. (1981). Free calcium ions in neurones of *Helix aspersa* measured with ion-selective micro-electrodes. *Journal of Physiology* **315**, 531–548.

Barish, M. E. & Thompson, S. H. (1983). Calcium buffering and slow recovery kinetics of calcium-dependent outward current in molluscan neurones. *Journal of Physiology* **337**, 201–219.

Belan, P., Kostyuk, P., Snitsarev, V. & Tepikin, A. (1993). Calcium clamp in isolated neurones of the snail *Helix pomatia*. *Journal of Physiology* **462**, 47–58.

Blumenfeld, H., Zablow, L. & Sabatini, B. (1992). Evaluation of cellular mechanisms for modulation of calcium transients using a mathematical-model of fura-2 Ca^{2+} imaging in *Aplysia* sensory neurons. *Biophysical Journal* **63**, 1146–1164.

Brindley, F. J., Tiffert, T., Scarpa, A. & Mullins, L. J. (1977). Intracellular calcium buffering capacity in isolated squid axons. *Journal of General Physiology* **70**, 355–384.

Fontana, G. & Blaustein, M. P. (1993). Calcium buffering and free Ca^{2+} in rat brain synaptosomes. *Journal of Neurochemistry* **60**, 843–850.

Hodgkin, A. L. & Keynes, R. D. (1957). Movements of labelled calcium in squid giant axons. *Journal of Physiology* **138**, 253–281.

Johnson, B. D. & Byerly, L. (1993). Photo-released intracellular Ca^{2+} rapidly blocks Ba^{2+} current in *Lymnaea* neurons. *Journal of Physiology* **462**, 321–347.

Kennedy, H. J. & Thomas, R. C. (1995). Intracellular calcium and its sodium-independent regulation in voltage-clamped snail neurones. *Journal of Physiology* **484**, 533–548.

Kostyuk, P. G., Mironov, S. L., Tepikin, A. V. & Belan, P. V. (1989). Cytoplasmic free Ca in isolated snail neurons as revealed by fluorescent probe fura-2: Mechanisms of Ca recovery after Ca load and Ca release from intracellular stores. *Journal of Membrane Biology* **110**, 11–18.

McGuigan, J. A. S., Lüthi, D. & Buri, A. (1991). Calcium buffer solutions and how to make them: A do it yourself guide. *Canadian Journal of Physiology and Pharmacology* **69**, 1733–1749.

Meech, R. W. & Thomas, R. C. (1980). Effect of measured calcium chloride injections on the membrane potential and internal pH of snail neurones. *Journal of Physiology* **298**, 111–129.

Müller, T. H., Partridge, L. D. & Swandulla, D. (1993). Calcium buffering in bursting *Helix* pacemaker neurons. *Pflügers Archiv* **425**, 499–505.

Neher, E. & Augustine, G. J. (1992). Calcium gradients and buffers in bovine chromaffin cells. *Journal of Physiology* **450**, 273–301.

Nowycky, M. C. & Pinter, M. J. (1993). Time courses of calcium and calcium-bound buffers following calcium influx in a model cell. *Biophysical Journal* **64**, 77–91.

Partridge, L. D. (1994). Cytoplasmic Ca^{2+} activity regulation as measured by a calcium-activated current. *Brain Research* **647**, 76–82.

Purves, R. D. (1981). *Microelectrode Methods for Intracellular Recording and Ionophoresis*. Academic Press, London.

Roos, A. & Boron, W. F. (1980). The buffer value of weak acids and bases: Origin of the concept, and first mathematical derivation and application to physico-chemical systems. The work of M. Koppel and K. Spiro (1914). *Respiratory Physiology* **40**, 1–32.

Sala, F. & Hernandez-Cruz, A. (1990). Calcium diffusion modelling in a spherical neuron – relevance of buffering properties. *Biophysical Journal* **57**, 313–324.

Saleh, A. M., Rombola, G. & Batlle, D. C. (1991). Intracellular H^+ buffering power and its dependence on intracellular pH. *Kidney International* **39**, 282–288.

Schwiening, C. J., Kennedy, H. J. & Thomas, R. C. (1993). Calcium–hydrogen exchange by the plasma membrane Ca-ATPase of voltage-clamped snail neurons. *Proceedings of the Royal Society* B **253**, 285–289.

Schwiening, C. J., Kennedy, H. J. & Thomas, R. C. (1995). Intracellular calcium buffering power measured in snail neurones. *Biophysical Journal* **68**, A382.

Stuenkel, E. L. (1994). Regulation of intracellular calcium and calcium buffering properties of rat isolated neurohypophysial nerve endings. *Journal of Physiology* **481**, 251–271.

Thomas, R. C., Coles, J. A. & Deitmer, J. W. (1991). Homeostatic muffling. *Nature* **350**, 564.

Thomas, R. C. & Schwiening, C. J. (1992). Optical fibre fluorescence system for intracellular Ca^{2+}measurement: one lamp and filter wheel supplies 2 set-ups. *Journal of Physiology* **452**, 153*P*.

Werth, J. L. & Thayer, S. A. (1994). Mitochondria buffer physiological calcium loads in cultured rat dorsal root ganglion neurons. *Journal of Neuroscience* **14**, 348–356.

Werth, J. L., Zhou, B., Nutter, L. M. & Thayer, S. A. (1994). 2′,3′-Dideoxycytidine alters calcium buffering in cultured dorsal root ganglion neurons. *Molecular Pharmacology* **45**, 1119–1124.

White, R. J. & Reynolds, I. J. (1995). Mitochondria and Na^+/Ca^{2+} exchange buffer glutamate-induced calcium loads in cultured cortical neurons. *Journal of Neuroscience* **15**, 1318–1328.

Zhou, Z. A. & Neher, E. (1993). Mobile and immobile calcium buffers in bovine adrenal chromaffin cells. *Journal of Physiology* **469**, 245–273.

Acknowledgements

We are grateful to the MRC for support and to Helen Kennedy and Erwin Neher for comments on an early version of the manuscript.

Authors' email addresses

c.j.schwiening@bristol.ac.uk

roger.thomas@bristol.ac.uk

Received 14 June 1995; accepted 4 October 1995.